

Spatial distribution of dressed-photon–phonon confined by an impurity atom-pair in a crystal

M. Ohtsu¹, E. Segawa², K. Yuki³, and S. Saito⁴

¹Research Origin for Dressed Photon, 3-13-19 Moriya-cho, Kanagawa-ku, Yokohama, Kanagawa 221-0022, Japan

²Yokohama National University, 79-8 Tokiwadai, Hodogaya-ku, Yokohama, Kanagawa 240-8501, Japan

³Middenii, 3-3-13 Nishi-shinjuku, Shinjuku-ku, Tokyo 160-0023, Japan

⁴Kogakuin University, 2665-1, Nakano-machi, Hachioji, Tokyo 192-0015, Japan

Abstract

This paper analyzes the spatial distribution of a dressed-photon–phonon (DPP) that is confined by a boron (B) atom-pair in a silicon light-emitting diode by using a two-dimensional quantum walk model. It is confirmed that the DPP is confined by the B atom-pair, which is oriented along a direction perpendicular to that of the incident light propagation. The dependence of the confined DPP probability on the length of the B atom-pair is analyzed. The spatial distribution profile of the confined DPP is found to be asymmetric, which indicates photon breeding with respect to the photon momentum.

1. Introduction

Crystalline silicon (Si) has been a key material supporting the development of modern technology for more than half a century. However, because Si is an indirect-transition-type semiconductor, it has been considered to be unsuitable for light-emitting devices: Since the bottom of the conduction band and the top of the valence band in Si are at different positions in reciprocal lattice space, the momentum conservation law requires an interaction between an electron–hole pair and a phonon for radiative recombination; however, the probability of this interaction is very low.

Nevertheless, Si has been the subject of extensive study for the fabrication of light-emitting devices. These include studies using porous Si [1], a super-lattice structure of Si and SiO₂ [2], and so on, but the devices fabricated in these studies have significant problems, such as low efficiency, the need to operate at low temperature, complicated fabrication processes, and the difficulty of current injection.

In a recent breakthrough, the problems above were solved by using a dressed photon (DP) [3,4]. A DP is a quantum field created by the interaction between photons and electrons (or excitons) in a nanometer-sized particle. It is an off-shell field because its momentum has a large uncertainty due to its subwavelength size [5,6]. Furthermore, DP couples with a phonon to create a new quantum field,

named a dressed-photon–phonon (DPP). The phonon, coupled with the DP, exchanges its momentum with the electron to follow the momentum conservation law, resulting in a resolution to the problem above and in successful fabrication/operation of light emitting diodes (LEDs) and lasers by using crystalline Si.

This paper analyzes the spatial distribution of a DPP confined by an impurity atom-pair (boron (B) atom-pair) in a Si-LED by using a two-dimensional quantum walk (QW) model. The analysis results are compared with experimental results for confirming the validity of using this model.

2. Experimental results for quantum walk analyses

To fabricate a Si-LED, the surface of an n-type Si crystal is transformed to a p-type semiconductor by implanting B atoms, forming a p-n homojunction (the ratio of the number of B atoms to that of the Si atoms is as low as 10^{-6}). This crystal is processed by a unique fabrication method named DPP-assisted annealing [3,4]: By current injection, Joule heat is generated, which causes the B atoms to diffuse (Fig. 1(a)). During this Joule-annealing, the Si crystal surface is irradiated with light (Fig. 1(b)). The light reaches the p-n homojunction to create a DP on the B atom, and the created DP localizes at the B atom. If the separation between two B atoms is sufficiently short, a phonon is confined by this B atom-pair. As a result, a new quantum field (DPP) is created due to the DP-phonon coupling and is confined by the B atom-pair. The phonon in the created DPP can provide momentum to the electron nearby to satisfy the momentum conservation law, resulting in radiative recombination for photon emission (Fig. 1(c)). This is stimulated emission triggered by the irradiated light. The emitted light propagates out from the crystal to the outside, which indicates that a part of the Joule energy used for diffusing the B atoms is dissipated in the form of optical energy, resulting in local cooling that locally decreases the diffusion rate. As a result, by the balance between heating by the Joule energy and cooling by the stimulated emission, the spatial distribution of B atoms varies and reaches a stationary state autonomously, fixing the direction and length of the B atom-pair. This stationary state is the optimum for efficient creation of the DPPs and for efficient LED operation because the probability of spontaneous emission is proportional to that of the stimulated emission described above.

It has been experimentally confirmed that, when the direction of the B atom-pair is perpendicular to that of the irradiated light propagation, the DPP creation probability is higher than the case of other orientation directions of the B atom-pair, including the parallel orientation [7]. The vertical axis in Fig. 2 indicates the difference ΔN in the number of B atom-pairs (along the perpendicular direction) after and before the DPP-assisted annealing, as acquired by atom probe field ion spectroscopy with sub-nanometer spatial resolution [8]. The horizontal axis indicates the ratio d/a between the length d of the pair and the lattice constant a of the Si crystal. Closed circles show that the value of ΔN takes the maximum at $d/a=3$. It should be noted that the value of d/a at this maximum depends on the density of the B atoms doped prior to the DPP-assisted annealing, which decreases with increasing density of the doped B atoms.

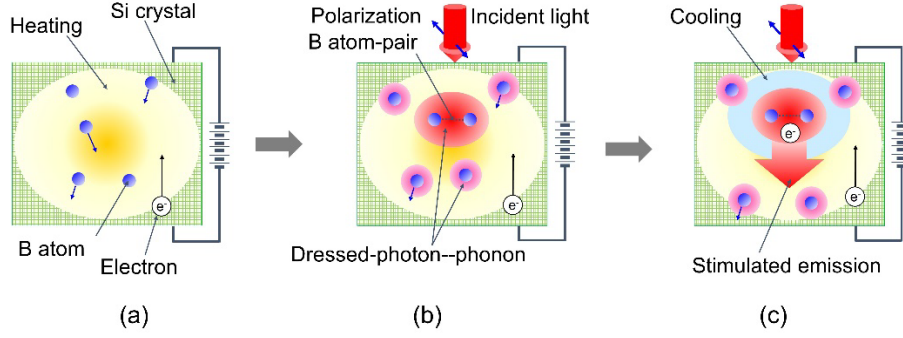


Fig. 1 DPP-assisted annealing.

(a) Diffusing B atoms by Joule heat. (b) Creating and localizing DP at B atom-pair. (c) Stimulated emission of photons.

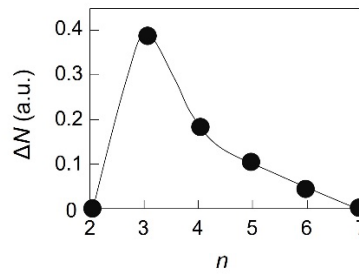


Fig. 2 Relation between the ratio d/a and the difference ΔN in the number of the B atom-pairs (along the perpendicular direction) after and before the DPP-assisted annealing.

3. Geometric model for numerical calculations

Numerical calculations are carried out for the cases of a single B atom (Fig. 3(a)), a B atom-pair that is oriented along directions perpendicular (Fig. 3(b)), and parallel (Fig. 3(c)) to the direction of the incident light propagation. It should be noted that experiments have confirmed that the DPP creation probability is the highest in the case of Fig. 3(b).

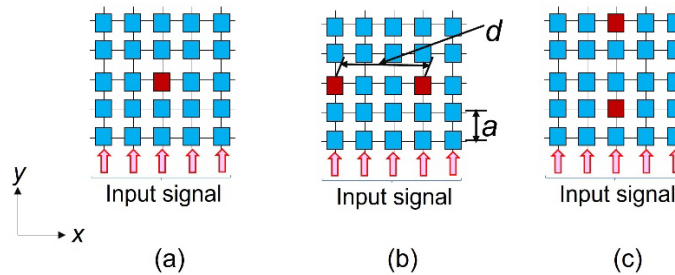


Fig. 3 Positions of B atoms in the square lattice of a Si crystal.

Red and blue closed squares represent the sites of B and Si atoms, respectively.

(a) A single B atom. (b), (c) B atom-pairs oriented along the directions perpendicular and parallel to that of the incident light propagation (named B atom-pairs (x) and (y)), respectively.

Reference [9] reported calculated results of the DPP creation probability in a fiber probe by using a two-dimensional QW model. The present paper uses a QW model that is equivalent to that of ref. [9]: As a geometric model, the square lattice in Fig. 4(a) is used simply because the size of the Si crystal is much larger than the length of the B atom-pair. By radiating light (an input signal that propagates along the y -axis) to the lower side of this lattice, DPs are created at the sites in the lattice and travel in the upper-right or lower-left directions. These directions correspond to directions parallel and antiparallel (along the y and $-y$ axes, respectively) to the direction of the irradiated light propagation. The QW model deals with the DP hopping to the nearest-neighbor site, and these directions are represented by red and blue bent arrows, respectively, in Fig. 4(b). The phonon is represented by a green loop because it does not exhibit the hopping due to its nonlocalized nature.

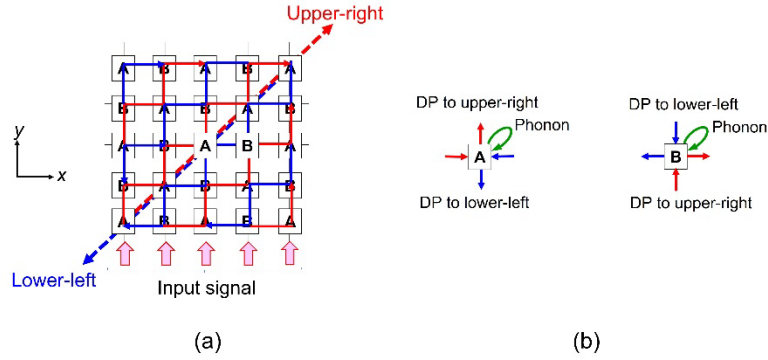


Fig. 4 Two-dimensional square lattice.

- (a) DPs that travel in the upper-right and lower-left directions. They are represented by bent red and blue arrows, respectively. (b) The magnified figure at sites A and B in (a). The green loop represents a phonon.

Since the DPP is a quantum field that is created as a result of coupling between two counter-travelling DPs and a phonon, a vector

$$\vec{\psi}_{t,(x,y)} = \begin{bmatrix} y_{DP+} \\ y_{DP-} \\ y_{Phonon} \end{bmatrix}_{t,(x,y)} \quad (1)$$

is used to express its creation probability amplitude, where $[\]$ is the vector at time t and at the position of the lattice site (x, y) , y_{DP+} and y_{DP-} are the creation probability amplitudes of the DPs that travel by repeating the hopping in the upper-right and lower-left directions, respectively, and y_{Phonon} is that of the phonon.

Spatial-temporal evolution equations for sites A and B in Fig. 4(b) are

$$\vec{\psi}_{t+1,(x,y)} = P_+ \vec{\psi}_{t,(x-1,y)} + P_- \vec{\psi}_{t,(x+1,y)} + P_0 \vec{\psi}_{t,(x,y)}, \quad (2)$$

and

$$\vec{\psi}_{t+1,(x,y)} = P_+ \vec{\psi}_{t,(x,y-1)} + P_- \vec{\psi}_{t,(x,y+1)} + P_0 \vec{\psi}_{t,(x,y)}, \quad (3)$$

respectively [10]. The sum of the coefficient matrices on the right-hand sides of these equations is

$$U = P_+ + P_- + P_0 = \begin{bmatrix} \varepsilon_+ & J & \chi \\ J & \varepsilon_- & \chi \\ \chi & \chi & \varepsilon_0 \end{bmatrix}, \quad (4)$$

which meets a unitary requirement for the QW model. Its diagonal elements ε_+ and ε_- are the eigen-energies of the DPs that travel to the upper-right and lower-left positions, respectively, and ε_0 is that of the phonon. Off-diagonal elements J and χ represent the DP hopping energy and the DP-phonon coupling energy, respectively. Since the DP couples with the phonon preferably at the B atom site, the value of χ at this site is fixed to be larger than J . On the other hand, $\chi = J$ at the Si atom site, as was the case in ref. [9]

The DPP reflection at the side of the square lattice can be neglected because the size of the Si crystal is much larger than the length of the B atom-pair*. To maintain the accuracy of approximating the Si crystal by the geometric square lattice model, the numbers n of the sites on the sides of the square lattice are increased to 51, as was employed in ref. [9].

(*) In ref. [9], the real-valued matrix in eq. (4) was replaced by a complex-valued unitary matrix $U(\xi) = \exp(i\xi)U$. As a result, this paper succeeded in analyzing the interference between the DPP reflected from the taper of the fiber probe and that created by the incident light. However, the present paper does not require this replacement because the reflection of the DPP at the sides of the square lattice is neglected.

4. Calculated results

4.1. Dependence on the direction of the B atom-pair

Figures 5(a) and (b) show the calculated dependences of the stationary spatial distribution of the DPP creation probability $|\vec{\psi}_{t,(x,y)}|^2$ in the square lattice ($n=51$) on the direction of the B atom-pair. They are the results for $d/a=3$. The value of χ/J at the B atom is fixed to be 10 and 20, respectively.

The left and right figures are for the perpendicularly and parallelly oriented B atom-pairs, respectively, (named B atom-pairs (x) and (y)). By comparing the DPP creation probabilities at the Si atoms between the two B atoms (two red open squares at the central part of these figures), it is found that the values of the probabilities for the B atom-pair (x) are larger than those for the B atom-pair (y). For more detailed comparison, spatial distributions of the DPP creation probability at the B atom-pairs (x) and (y) are shown by closed and open circles in Figs. 6(a)-(d), respectively, for which the values of χ/J at the B atom are 5, 10, 15, and 20. The value of d/a is varied from 1 to 5. For reference, the results for the cases of a single B atom ($d/a=0$) are also shown. From the large values represented by closed circles, it is confirmed that the DPP is effectively confined by the B atom-pair (x), as shown by the left figures in Figs. 5(a) and (b). The small values represented by open circles indicate that the DPP is not effectively confined by the B atom-pair (y) (the right figures in Figs. 5(a) and (b)). These orientation-dependences agree with the experimental results reviewed at the end of Section 2. Figures 6(a)–(d) also show that the probability distributions, represented by the closed circles, are asymmetric. The origin of this will be discussed using Fig. 10 in the next subsection.

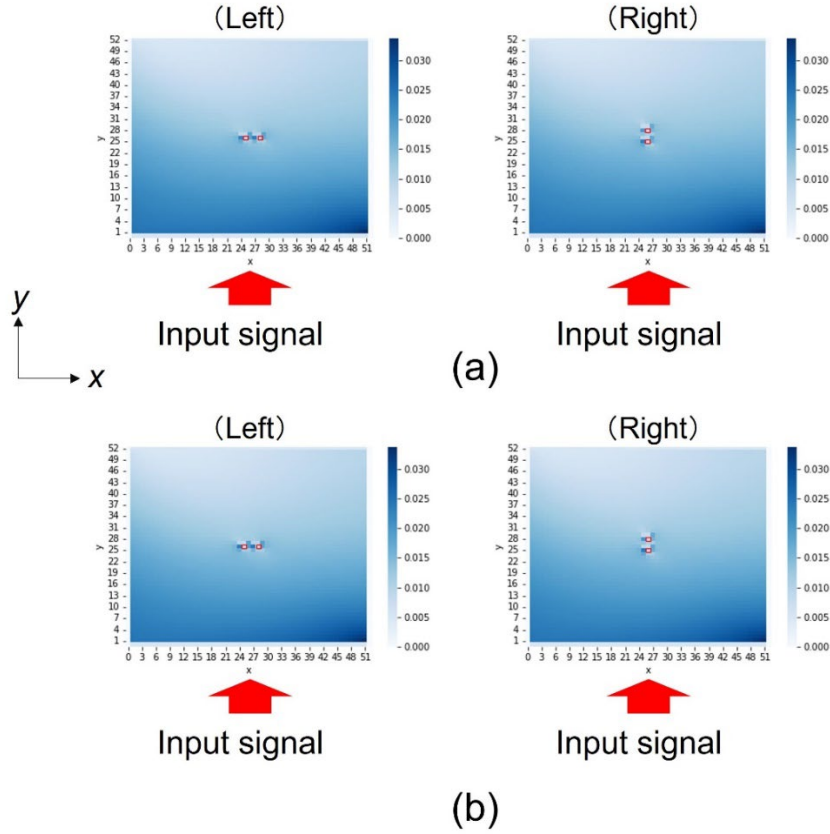


Fig. 5 Spatial distribution of the DPP creation probability for all the sites in the square lattice ($n=51$ and $d/a=3$). Two red open squares at the center represent the positions of the two B atoms. In (a) and (b), the value of χ/J at the B atom is fixed to be 10 and 20, respectively. Left and right figures represent the spatial distributions for the B atom-pairs (x) and (y), respectively.

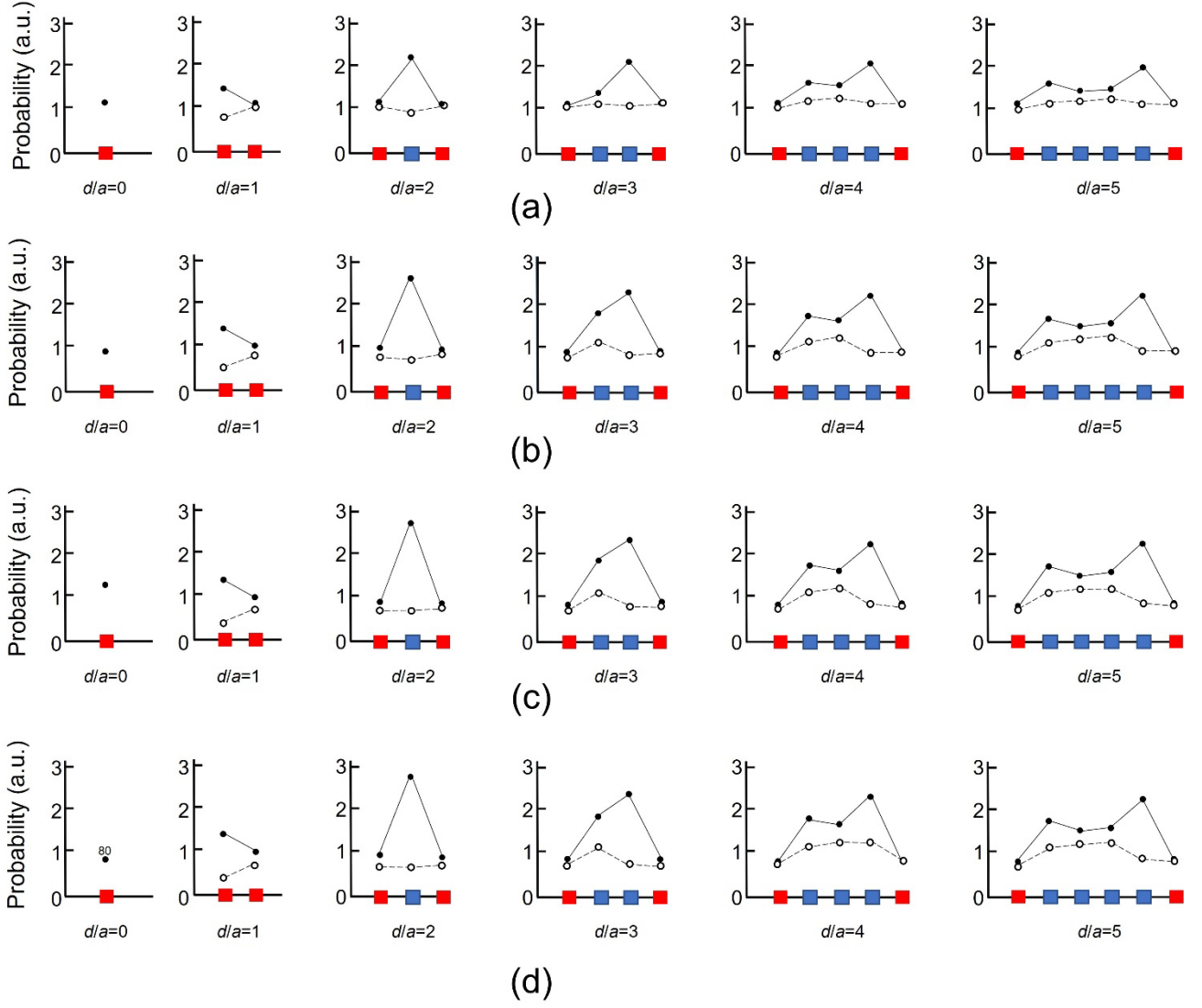


Fig. 6 Cross-sectional spatial distributions of the DPP creation probability along the x - and y -axes, represented by closed and open circles, respectively. Red and blue closed squares represent the sites of the B and Si atoms. The value of d/a is varied from 1 to 5. The value $d/a=0$ denotes that a single B atom exists in the lattice. In (a)–(d), the values of χ/J at the B atom are 5, 10, 15, and 20.

Two measures (1) and (2) are used to evaluate the confinement above:

- (1) The DPP creation probability C_{av} , averaged over all the sites in the B atom-pair (Fig. 7): It is expressed as $C_{av} \equiv A_{av} - B_{av}$. Here, A_{av} is the DPP creation probability, averaged over the Si atoms between the two B atoms. B_{av} is the average for the sites of the two B atoms.
- (2) The DPP creation probability C_T , integrated over all the sites in the B atom-pair (Fig. 8): It is

expressed as $C_T = ((d/a) - 1)C_{av}$.

Figure 7 shows that the value of C_{av} takes the maximum at $d/a = 2$ and decreases monotonically with the increase of d/a , which agrees with the experimental results in Fig. 2*. Figure 8 shows that the value of C_T increases monotonically with the increase of d/a , which is due to the contribution from $(d/a) - 1$ in C_T . These two figures also show that the values of C_{av} and C_T do not strongly depend on χ/J when $\chi/J \geq 10$.

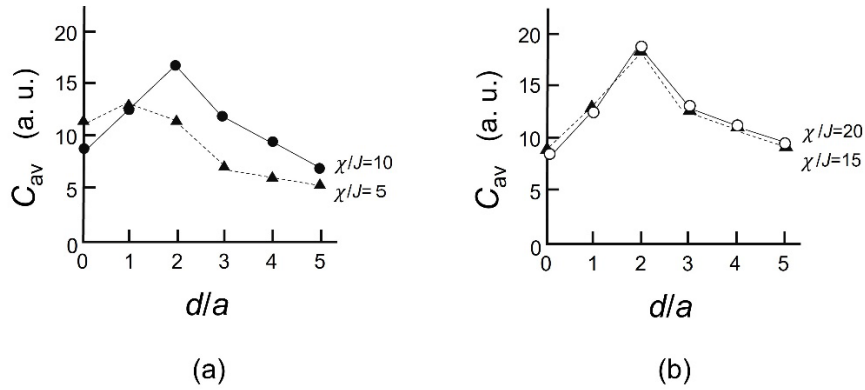


Fig. 7 The dependence of C_{av} on d/a .

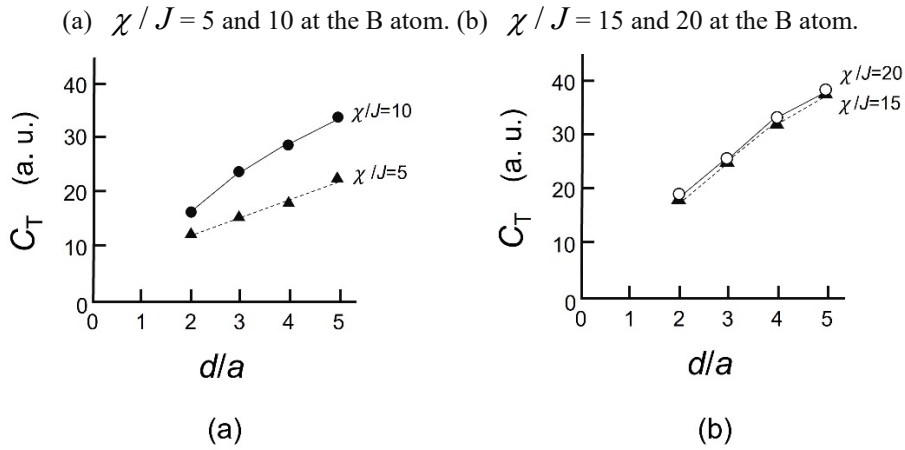


Fig. 8 The dependence of C_T on d/a .

(a) $\chi/J = 5$ and 10 at the B atom. (b) $\chi/J = 15$ and 20 at the B atom.

(*) Although Fig. 2 shows that the value of ΔN takes the maximum at $d/a=3$, this maximum value is apt to fluctuate, depending on the density fluctuations of the B atoms doped into the Si crystal prior to the DPP-assisted annealing. Thus, it can be claimed that Fig. 7 agrees with Fig. 2.

4.2. Asymmetric distribution and photon breeding

Since closed circles in Fig. 6 shows that DPP is effectively confined by the B atom-pair (x), the present subsection presents the calculated results only for the B atom-pair (x). Figure 9 shows the calculated results for all the sites in the square lattice ($n=51$, $d/a=3$, and $\chi/J=20$ at the B atoms). Figure 9(a) is for $|\vec{\psi}_{t,(x,y)}|^2$, which corresponds to the left figures in Fig. 5. Figure 9(b) shows that the values of $|y_{DP+}|^2$ in the broken rectangular area are much larger than those of $|y_{DP-}|^2$ in the same rectangular area of Fig. 9(c). This means that the DP creation probability $|y_{DP+}|^2$, travelling in the same direction as that of the incident light propagation (along the y -axis), is larger. In other words, the DP creation probability, traveling in the same direction as that of the incident photon momentum, is larger. This indicates the presence of photon breeding (PB) with respect to the photon momentum [4].

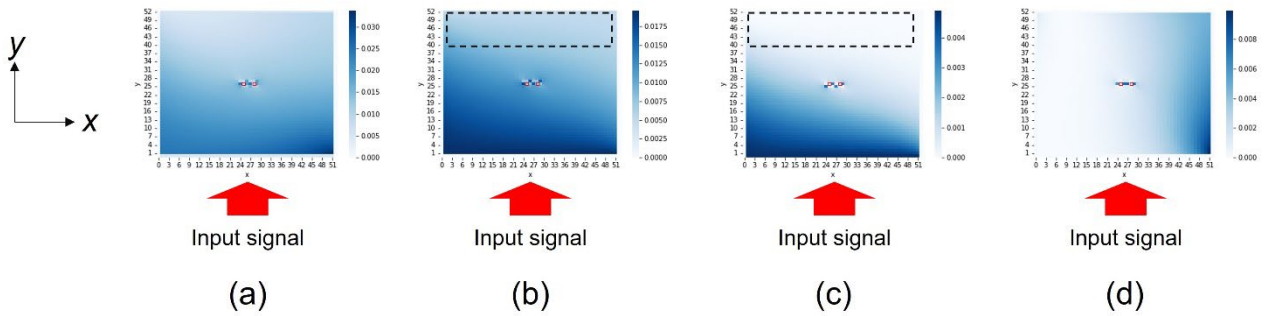


Fig. 9 Spatial distributions of the creation probabilities for all the sites in the square lattice ($n=51$, $d/a=3$, and $\chi/J=20$ at the B atom). (a) $|\vec{\psi}_{t,(x,y)}|^2$, (b) $|y_{DP+}|^2$, (c) $|y_{DP-}|^2$, and (d) $|y_{Phonon}|^2$.

Calculated probabilities $|y_{DP+}|^2$, $|y_{DP-}|^2$, and $|y_{Phonon}|^2$ at the B atom-pair (x) are shown in Figs. 10(a), (b), and (c), respectively. Here, χ/J at the B atom is fixed to 20. The value of $|y_{DP+}|^2$ (Fig. 10(a)) is larger than that of $|y_{DP-}|^2$ (Fig. 10(b)), which again indicates PB, as was pointed out above.

Furthermore, the distributions of $|y_{DP+}|^2$ and $|y_{DP-}|^2$ are asymmetric in spite of the symmetric

distribution of the phonon $|y_{Phonon}|^2$ (Fig. 10(c)). This asymmetry is clearly seen for $d/a \geq 3$. In Fig. 10(a), the value of $|y_{DP+}|^2$ at the Si atom on the right is larger than that on the left. In contrast, in Fig. 10(b), the value of $|y_{DP-}|^2$ at the Si atom on the left is larger. From this contrast, it is concluded that the asymmetry in $|\vec{\psi}_{t,(x,y)}|^2$ (closed circles in Fig. 6) originates from that in $|y_{DP+}|^2$ of Fig. 10(a).

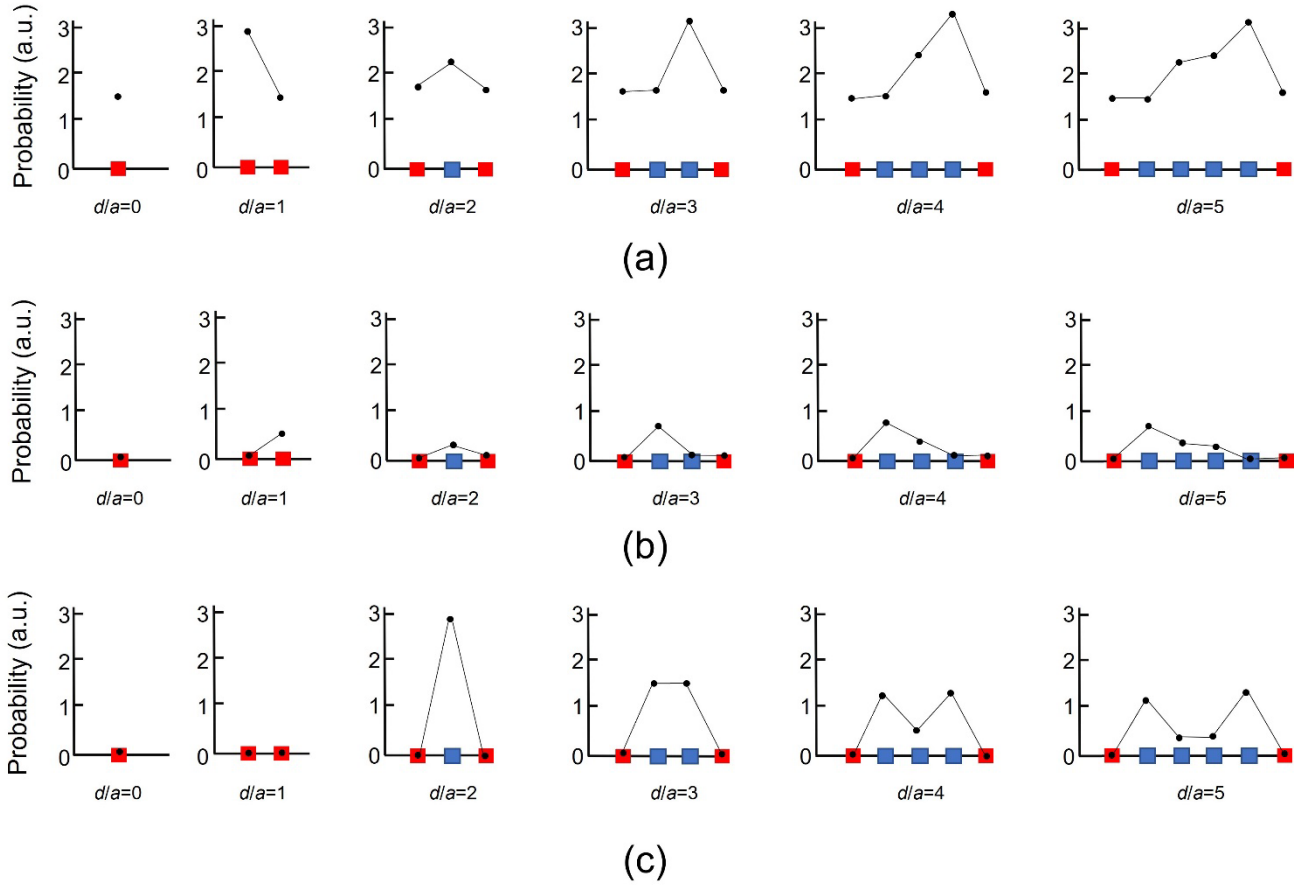


Fig. 10 Cross-sectional spatial distributions of the creation probabilities of DP and phonon. The value of d/a is varied from 1 to 5. $\chi/J=20$ at the B atom (red closed square).

(a) and (b) are for $|y_{DP+}|^2$ and $|y_{DP-}|^2$, respectively. (c) is for $|y_{Phonon}|^2$.

5. Summary

This paper analyzed the spatial distribution of a DPP that is confined by a B atom-pair in a Si-LED by using a two-dimensional quantum walk (QW) model. The results of the calculation are:

- (1) The DPP is confined by the B atom-pair that is oriented along a direction perpendicular to that of the incident light propagation. This orientation-dependence agrees with the experimental results.
- (2) The value of the creation probability of the confined DPP takes the maximum at $d/a=2$ and decreases monotonically with the increase of d/a . This length-dependence agrees with the experimental results.
- (3) The spatial distribution profile of the creation probability of the confined DPP is asymmetric. This is because the DP creation probability, travelling in the same direction as that of the light incident, is larger. This indicates PB with respect to the photon momentum.

Advanced numerical calculations including the energy dissipation of the DPP confined in a B atom-pair are planned. Future analyses of PB with respect to the photon spin (polarization) [11] by a three-dimensional QW model are also planned.

References

- [1] Hirschman, K.D., Tysbekov, L., Duttagupta, S.P., & Fauchet, P.M., Silicon-based visible light emitting devices integrated into microelectronic circuits. *Nature*, **384**, 338-341, (1996).
- [2] Lu, Z.H., Lockwood, D.J., & Baribeau, J.M, Quantum confinement and light emission in SiO₂/Si superlattices. *Nature*, **378**, 258–260, (1995).
- [3] Kawazoe, T., Mueed, M.A. & Ohtsu, M. Highly efficient and broadband Si homojunction structured near-infrared light emitting diodes based on the phonon-assisted optical near-field process, *Appl. Phys.B*, **104**, 747-754 (2011).
- [4] Ohtsu, M., *Silicon Light-Emitting Diodes and Lasers*, (Springer, Heidelberg, 2016) pp.1-13.
- [5] Ohtsu, M., Ojima, I., and Sakuma, H., “Dressed Photon as an Off-Shell Quantum Field,” *Progress in Optics* Vol.64, (ed. T.D. Visser) pp.45-97 (Elsevier, 2019).
- [6] M. Ohtsu, *Off-Shell Applications In Nanophotonics*, Elsevier, Amsterdam (2021) p.5.
- [7] Ohtsu, M., *Silicon Light-Emitting Diodes and Lasers*, (Springer, Heidelberg, 2016) pp.38-39.
- [8] Ohtsu, M., *Silicon Light-Emitting Diodes and Lasers*, (Springer, Heidelberg, 2016) pp.35-36.
- [9] Ohtsu, M., Segawa, E., Yuki, K., and Saito, S., ““Dressed-photon—phonon creation probability on the tip of a fiber probe calculated by a quantum walk model,” *Off-shell Archive* (December, 2022) OffShell: 2212O.001.v1., DOI 10.14939/2212O.001.v1, https://rodrep.or.jp/en/off-shell/original_2212O.001.v1.html
- [10] Ohtsu, M., Segawa, E., and Yuki, K., “Numerical calculation of a dressed photon energy transfer based on a quantum walk model,” *Off-shell Archive* (June, 2022) OffShell: 2206O.001.v1., DOI10.14939/2206O.001.v1, https://rodrep.or.jp/en/off-shell/original_2206O.001.v1.html
- [11] Ohtsu, M., *Silicon Light-Emitting Diodes and Lasers*, (Springer, Heidelberg, 2016) pp.39-42.